Method of Sensor Noise Attenuation in High–Gain Observers — Experimental Verification on Two Laboratory Systems

Rafał Madoński* and Przemysław Herman

Abstract— **In this paper, a measurement noise attenuation technique is applied to a state observer in order to decouple the noise from the estimated state variables. It is important to limit such interferences, since the estimates are: 1) used online to formulate the state feedback controller, and 2) used in the compensation loop, where the estimated overall uncertainty of the system is partially canceled from the original plant. This measurement noise rejection method, which is based on extending the plant model with an additional, integral state variable, allows user to choose higher gains of the observer in order to provide faster convergence of its estimates, without the danger of making the system less energy-effective (or even destabilizing it) due to noise amplification. Experiments, conducted on two laboratory testbeds, show that the considered technique gives satisfactory results in practical application.**

I. Introduction

The high-gain observers (HGO) are well-known and popular techniques for fast and reliable state reconstruction (a survey can be found in [8]). An interesting class of HGOs, which is currently receiving considerable attention by both the control theorists and practitioners, is the one that extends the nominal model of the plant with additional, fictitious state variables that represent the overall perturbation in the system (a sum of modeling uncertainty and external disturbance - often referred in literature as the *total disturbance*). These states are then estimated by the observer and used in the feedback loop to compensate for the actual interferences in the system. Such techniques greatly simplify the control problem since they limit the influence of the unmodeled effect in the considered process. Examples of such methods include: Extended State Observer (ESO) [2], Generalized Proportional Integral Observer (GPI) [6], or Extended High–Gain Observer [3]. In order to give satisfactory results, the HGOs need their gains to be sufficiently high to provide rapid and accurate estimation of the state variables. Choosing large gains may however turn out to be problematic in engineering practice for two following reasons.

The first one is the *peaking phenomenon*, which corresponds to a huge estimation error during a short period of time, right after the initial time or the moment when the output is changed suddenly. There are many techniques to limit this effect, yet the simplest one (but not the most effective) is the saturation of the estimation error. The peaking behavior is however beyond the scope of this paper, but its thorough examination can be found in [10].

*R. Madoński and P. Herman are with the Chair of Control and Systems Engineering, Faculty of Computing, Poznań University of Technology, ul. Piotrowo 3a, 61-138, Poznań, Poland rafal.madonski@doctorate.put.poznan.pl, przemyslaw.herman@put.poznan.pl

The second reason is the measurement noise, which is inevitable in practical applications. It usually results from the faulty nature of measuring devices. Since the HGOs use the control signal and the output signal of the plant, the user, by increasing the observer gains, also amplifies the noise in the state estimates. Such noisy signals, when used in the feedback or compensation loops may even destabilize the closed-loop system if the noise is sufficiently large. Thus, the need is to find a solution that will not only provide accurate estimates of the system states, but will guarantee smooth and disturbance-free signal profiles.

A potential solution to the problem of noise amplification in the observer output lies in the work dedicated to Proportional Integral Observers (PIO, see [1] and references therein) in which an additional term (proportional to the integral of the output estimation error) is introduced to the system to achieve some desired robustness performance. Strictly speaking, this term is used as an additional degree of the observer in order to decouple the sensor noise. In [6], authors combined this *integral state* with the GPI observer, however only numerical simulations were presented there.

Hence, the goal of this paper is to verify if the known measurement noise attenuation theory can be successfully implemented in practice[1]. The contribution of the work is the experimental verification of the disturbance-rejection control technique that assumes an expansion of the system with two, additional, fictitious state variables. First one represents the *total disturbance*, and the other one is used as a noise decoupling mechanism. In this work, the linear version of the high-gain ESO, along with a state feedback controller, is used. Such approach is similar to Active Disturbance Rejection Control (or ADRC [2]), however the difference is that the ADRC extends the observer only with state variables representing the *total disturbance*. We will denote the proposed technique as ADRC* in order to distinguish the considered method from the classical version of ADRC.

II. Problem formulation

A following second order system is considered:

$$\ddot{q} = \overbrace{f_{int}(q,\dot{q},\ldots) + f_{ext}(\cdot)} + bu = f(q,\dot{q},\ldots) + bu, \quad (1)$$

where $u \in \mathbb{R}$ is the input signal, $q \in \mathbb{R}$ is the output signal, $f_{int}(\cdot) \in \mathbb{R}$ denotes the plant internal dynamics, $f_{ext}(\cdot) \in$

[1]Two laboratory setups are used for the experiments to make the conclusions more credible, since the systems differ from each other in terms of type and relative order of the dynamics as well as the characteristics of their sensor devices.

978-1-4673-2706-0/12/$31.00 ©2012 IEEE

$\mathbb{R}$ stands for the external disturbance, and $b \in \mathbb{R}$ is the system unknown parameter. By merging the unknown plant dynamics with the external disturbance into one element, the above plant was rewritten using $f(\cdot) \in \mathbb{R}$, which is the unknown *total disturbance*[2].

By assuming a set of phase state variables (i.e. $z_1 = q \Rightarrow \dot{z}_1 = z_2 = \dot{q}$), the system from (1) can be alternatively defined as:

$$\begin{cases} \dot{z}_1 = z_2, \\ \dot{z}_2 = f(\cdot) + bu, \quad \text{for } q = z_1, \end{cases} \tag{2}$$

where the *total disturbance* could be easily obtained by solving the equation:

$$f(\cdot) = \dot{z}_2 - bu, \tag{3}$$

however, in order to do that, the user would have to provide information about the state $\dot{z}_2$ and the parameter b, which is often problematic from a practitioner point of view.

The ADRC-type methods however, are based on an idea that as long as the $f(\cdot)$ is estimated closely in real time, analytical expression of the *total disturbance* is not required. In the ADRC approach, the ESO is proposed as a method for estimating $f(\cdot)$. To introduce it, the state space model (2) is first artificially extended to:

$$\begin{cases} \dot{z}_1 = z_2, \\ \dot{z}_2 = z_3 + bu, \\ \dot{z}_3 = \dot{f}(\cdot), \end{cases} \tag{4}$$

where the additional state variable $z_3 = f(\cdot)$ represents the user-defined *total disturbance*. All three states can be now estimated with a third order linear ESO, which is defined as:

$$\begin{cases} \dot{\hat{z}}_1 = \hat{z}_2 + L_1\varepsilon, \\ \dot{\hat{z}}_2 = \hat{z}_3 + L_2\varepsilon + \hat{b}u, \\ \dot{\hat{z}}_3 = L_3\varepsilon, \end{cases} \overset{aim}{\Longrightarrow} \begin{cases} \hat{z}_1 \to q, \\ \hat{z}_2 \to \dot{q}, \\ \hat{z}_3 \to f(\cdot), \end{cases} \tag{5}$$

where L_1, L_2, $L_3 > 0$ are the observer gains, $\varepsilon \triangleq z_1 - \hat{z}_1 = q - \hat{z}_1$ is the estimation error of state z_1, $\hat{b}$ is the constant value, approximation of b from equation (1), and $\hat{z}_1$, $\hat{z}_2$, $\hat{z}_3$ are the estimates of state variables z_1, z_2, z_3, respectively.

The estimation error dynamics is given in such approach as:

$$\varepsilon^{(3)} + L_1\ddot{\varepsilon} + L_2\dot{\varepsilon} + L_3\varepsilon = \dot{f}(\cdot), \tag{6}$$

where notation $\varepsilon^{(i)}$ means the i-th time derivative. As proved in [11], if $f(\cdot)$ is absolutely and uniformly bounded by a constant and positive parameter, it is possible to choose the L_1-L_3 coefficients in such a way that the observation error converges asymptotically to the neighborhood of zero.

Things get more complicated when the system output signal is affected by the noise measurement, which cannot be effectively estimated as a part of the *total disturbance*. Such plant can be described as:

$$\begin{cases} \dot{z}_1 = z_2, \\ \dot{z}_2 = f(\cdot) + bu, \quad \text{for } q = z_1 + d, \end{cases} \tag{7}$$

for the output of the system being defined as $q = z_1 + d$, where d is the measurement noise that corrupts the output signal (cf. (2)). Now, the estimation error dynamics from (6) takes a following new form:

$$\begin{aligned} \varepsilon^{(3)} + L_1\ddot{\bar{\varepsilon}} + L_2\dot{\bar{\varepsilon}} + L_3\bar{\varepsilon} \quad &= \\ = \dot{f}(\cdot) + d^{(3)} - L_1\ddot{d} - L_2\dot{d} - L_3 d. & \end{aligned} \tag{8}$$

where $\varepsilon \triangleq q - \hat{z}_1 = z_1 + d - \hat{z}_1 = \bar{\varepsilon} + d$. It is clear that the dynamics of the measurement noise is now affected proportionally with the observer gains and, in the case that they would be of high magnitude, this scaled dynamics affects the observer convergence. Thus, this may not bring satisfactory performance while dealing with significant sensor noise.

A. Proposed solution

In order to deal with noisy measurements, the ESO structure can be augmented with another fictitious state variable, defined as: $z_0 \triangleq \int_0^t q(\tau)d\tau = \int_0^t [z_1(\tau) + d(\tau)]\,d\tau$, which is the integrated output signal from (7). The reformulated plant, with extra state variables (z_0 which is the *integral* state, and z_3 which represents the *total disturbance*) can be now described as seen below:

$$\begin{cases} \boxed{\dot{z}_0 = z_1 + d,} \\ \dot{z}_1 = z_2, \\ \dot{z}_2 = z_3 + bu, \\ \dot{z}_3 = \dot{f}(\cdot). \end{cases} \tag{9}$$

The new ESO observer (cf. (5)) for the considered second order system in (1), but with two extra state variables, is designed as follows:

$$\begin{cases} \dot{\hat{z}}_0 = \hat{z}_1 + L_0\varepsilon_0, \\ \dot{\hat{z}}_1 = \hat{z}_2 + L_1\varepsilon_0, \\ \dot{\hat{z}}_2 = \hat{z}_3 + L_2\varepsilon_0 + \hat{b}u, \\ \dot{\hat{z}}_3 = L_3\varepsilon_0, \end{cases} \overset{aim}{\Longrightarrow} \begin{cases} \hat{z}_0 \to z_0, \\ \hat{z}_1 \to q, \\ \hat{z}_2 \to \dot{q}, \\ \hat{z}_3 \to f(\cdot), \end{cases} \tag{10}$$

where $\varepsilon_0 \triangleq z_0 - \hat{z}_0$. The estimation error dynamics for the above observer is presented below:

$$\varepsilon_0^{(4)} + L_0\varepsilon_0^{(3)} + L_1\ddot{\varepsilon}_0 + L_2\dot{\varepsilon}_0 + L_3\varepsilon_0 = \dot{f}(\cdot) + d^{(3)}. \tag{11}$$

The noise dynamics is now less affected by the observer gains, especially by the scaled noise dynamics $d^{(3)} + L_1 d^{(2)} + L_2 d^{(1)} + L_3 d$ seen in (9). Such approach is similar to the integrating action known from a classic PID controller. This procedure partially decouples the noise dynamics from the observer gains, thus improving the observer convergence without changing its gains (except one extra gain in ESO that needs tuning).

The control signal in both ADRC and ADRC* methods has to compensate the effects of the *total disturbance*,

[2]Note that the considered exemplary system is treated in this approach as a *grey box* model, where only the relative order of the plant and its I/O signals are assumed to be known. However, in general, if the user poses a reliable information about the mathematical representation of the plant (or part of it) one should incorporate this knowledge into the observer.

estimated by the ESO (i.e. $\hat{z}_3$ from (10)). It is usually defined as [2]:

$$u \triangleq \frac{-\text{estim. disturb.} + \text{feedback control sign.}}{\text{scaling parameter}} = \frac{-\hat{z}_3 + \bar{u}}{\hat{b}}, \tag{12}$$

where $\bar{u}$ is the output signal from the feedback controller (which type is usually chosen to a particular situation in order to guarantee the desired system behavior).

If the observer is ideally tuned (i.e. $\hat{z}_3 \approx f(\cdot)$ and $\hat{b} \approx b$), equation (7) with the new control signal (12) can be transformed to:

$$\ddot{q} \approx f(\cdot) + b\left(\frac{-\hat{z}_3 + \bar{u}}{\hat{b}}\right) \approx \bar{u}. \tag{13}$$

The plant model is now being desirably (yet theoretically) reduced to a double integrator form:

$$\begin{cases} \dot{z}_1 = z_2, \\ \dot{z}_2 = \bar{u}. \end{cases} \tag{14}$$

The ADRC* uses the noise-attenuation mechanism, therefore it limits the threat of destabilizing the observer by amplifying the noise with high gains. The considered approach also provides the dynamical compensation of the *total disturbance* and reduces the problem of governing a potentially nonlinear, time-varying system to a simpler control of a linear system. Thus, in some cases, even linear control techniques can be introduced to handle the complex process.

In the next section, the ADRC* technique is applied to two laboratory setups and compared to standard ADRC approach in order to verify its practical validity.

III. Laboratory Systems Description

A. Reel-to-reel mechanism (R2R)

The R2R system is a laboratory setup that simulates the reinforcement stage in a tire production process (Fig.1, for details see [5]). It can be described with a simplified physical model, where the first reel (R1) winds the reinforced rubber and the second one (R2) can be used to produce the external disturbance to the system. Both reels are driven with DC motors, where the input voltages are the input signals for the whole system. The main control task in the R2R setup is to wind the reinforced rubber in order to obtain the desired length (height) of the sag. Current length of the sag (L), which is the output signal from the system, is measured with a linear wire encoder placed on the upper base of R2R and attached to the load (M, it is also considered as the lowest point of the sag). The additional mass on the sag is a design parameter that can be interpreted as a weight of the winded rubber.

The mathematical model of the first order R2R plant is presented below (for more concrete information see [7]):

$$\dot{y} = \dot{y}_{R1} + \dot{y}_{R2}, \tag{15}$$

which can be further expanded and formulated as a *grey box* model:

$$\dot{y} = \frac{r\eta}{2}\omega(u_R) + \dot{y}_{R2} \overset{(1)}{\Longrightarrow} b_1 u_R + f(\cdot), \tag{16}$$

Fig. 1. The R2R laboratory setup with the assumed notation.

where $\dot{y}$[V/s] is the linear velocity of the mass (M) attached to the end of the sag, $\dot{y}_{R1}$ stands for the momentary, circumference velocity of the line winded by motor R1, $\dot{y}_{R2}$ is the momentary, circumference velocity of the line winded by motor R2 (external disturbance), r[m] denotes the time-dependent radius of the line winded up on the reel R1, $0 < \eta < 1$ is the transmission ratio, $\omega(u_R)$[rad/s] is the angular velocity of the motor R1 generated by the input voltage (u_R), and b_1 is the system unknown, time-varying parameter.

The system from (16) can be rewritten in the following state space form:

$$\begin{cases} \dot{x}_1 = b_1 u_R + f(\cdot), \\ y = x_1 + d, \end{cases} \tag{17}$$

where y[V] is the system output signal, corrupted with noise (d). The ESO in the ADRC*, for the first order R2R plant with two fictitious state variables (x_0 representing the *integral* state and x_2 being the assumed *total disturbance*), is designed as follows:

$$\begin{cases} \dot{\hat{x}}_0 = \hat{x}_1 + \alpha_0(x_0 - \hat{x}_0), \ \hat{x}_0(0) = 0, \\ \dot{\hat{x}}_1 = \hat{x}_2 + \alpha_1(x_0 - \hat{x}_0) + \hat{b}_1 u_R, \ \hat{x}_1(0) = y, \\ \dot{\hat{x}}_2 = \alpha_2(x_0 - \hat{x}_0), \ \hat{x}_2(0) = 0, \end{cases} \tag{18}$$

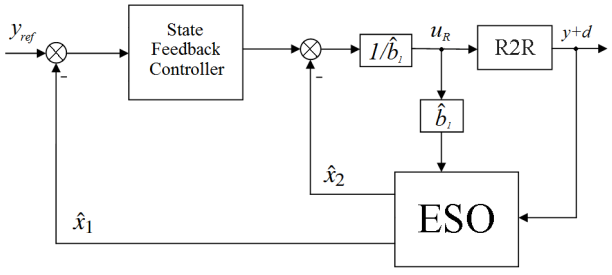

Fig. 2. A block diagram of the ZB2 control strategy.

where $x_0 = \int_0^t [y(\tau) + d(\tau)]\, d\tau$. In the ADRC-based approach, the control signal is defined as in (12):

$$u_R = \frac{-\hat{x}_2 + k_p \left(y_{ref} - \hat{x}_1\right)}{\hat{b}_1}, \tag{19}$$

in which $k_p > 0$ is the proportional gain of the state feedback controller and $y_{ref} \in (2,8)$[V] is the reference sag length.

B. Rotor system (TRAS)

The TRAS is an academic training setup used for various control experiments. Originally, the TRAS system is a two-input two-output plant, but in this study one degree-of-freedom is blocked mechanically and thus reduces it to a 1DOF plant. The TRAS setup contains a propeller, driven with a DC motor, located at the end of the rigid beam (Fig.3). The beam is fixed to a pivot point and thus can rotate freely in the horizontal plane. From the control point of view, TRAS is a single-input single-output system, where the motor voltage is the input signal for the system and the current yaw angle of the beam is the output signal (measured with a rotary encoder). The control objective is to keep the beam of the TRAS at the desired angle.

The simplified second order dynamics equations of the considered rotor system can be described as a following *grey box* model (for details see [4], [9]):

$$\ddot{\theta} = -\frac{k_c}{J_v}\dot{\theta} + \frac{k_s l_b}{J_v} F_p\left(\omega_m(u_m)\right) + d_{ext2} \overset{(1)}{\Longrightarrow} b_2 u_m + f(\cdot), \tag{20}$$

where θ[rad] is the yaw angle (i.e. around vertical axis) of the system beam, J_v[kgm^2] corresponds to the beam moment of inertia (relative to the vertical axis), k_c is the system parameter, k_s is the a scaling multiplier, l_b[m] stands for the length of beam from the propeller to the pivot point, d_{ext2} represents other and unknown disturbances acting on the system, and $F_p\left(\omega_m(u_m)\right)$[N] is the nonlinear function that represents the propeller thrust related to the angular velocity of the DC motor (ω_m[rad/s]) and the input voltage (u_m[V]) that runs it, and b_2 is the system design parameter.

By assuming the phase state variables (i.e. $\chi_1 = \theta \Rightarrow \dot{\chi}_1 = \chi_2 = \dot{\theta}$), the system from (20) can be rewritten in the following state space form:

$$\begin{cases} \dot{\chi}_1 = \chi_2, \\ \dot{\chi}_2 = f(\cdot) + b_2 u_m, \\ \theta = \chi_1 + d. \end{cases} \tag{21}$$

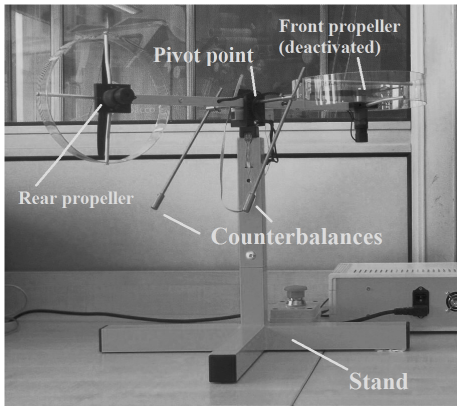

Fig. 3. The TRAS laboratory setup with the assumed notation.

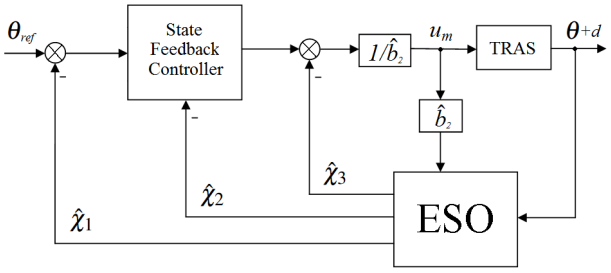

Fig. 4. A block diagram of the TRAS control strategy.

The ESO in the ADRC* for the second order TRAS plant, with two extra and fictitious state variables (χ_0 and χ_3), is designed as follows:

$$\begin{cases} \dot{\hat{\chi}}_0 = \hat{\chi}_1 + \beta_0\left(\chi_0 - \hat{\chi}_0\right), \ \hat{\chi}_0(0) = 0, \\ \dot{\hat{\chi}}_1 = \hat{\chi}_2 + \beta_1\left(\chi_0 - \hat{\chi}_0\right), \ \hat{\chi}_1(0) = \theta, \\ \dot{\hat{\chi}}_2 = \hat{\chi}_3 + \beta_2\left(\chi_0 - \hat{\chi}_0\right) + \hat{b}_2 u_m, \ \hat{\chi}_2(0) = 0, \\ \dot{\hat{\chi}}_3 = \beta_3\left(\chi_0 - \hat{\chi}_0\right), \ \hat{\chi}_3(0) = 0, \end{cases} \tag{22}$$

where $\chi_0 = \int_0^t [\theta(\tau) + d(\tau)]\, d\tau$. The control signal is defined as in (4):

$$u_m = \frac{-\hat{\chi}_3 + k_p\left(\theta_{ref} - \hat{\chi}_1\right) - k_d \hat{\chi}_2}{\hat{b}_2}, \tag{23}$$

in which $k_p > 0$ and $k_d > 0$ are the proportional and the derivative gains of the state feedback controller respectively, and $\theta_{ref} \in (-\pi, \pi)$[rad] is the desired beam angle.

IV. Experiments

A. Study preparation

In the conducted tests, a *grey box* approach is considered, which means that only the relative orders of the systems as well as their input and output information is given. In both R2R and TRAS setups, the whole dynamic behavior of the plant including the external perturbation is considered to be unknown, hence treated as the *total disturbance* in the ADRC-type techniques. In the experiments, the ADRC* method is compared to traditional ADRC in terms of estimation quality and energy-efficiency of the control mechanism.

The R2R and TRAS systems are operated from a standard PC via real-time I/O cards. The user-machine interface is realized through the popular engineering software tools - ViSim (R2R) and Matlab/Simulink (TRAS). The sampling times of the laboratory setups are set to $T_{s1} = 0.001$s and $T_{s2} = 0.005$s for the R2R and the TRAS systems, respectively.

The observer gains are chosen as follows. In the case of R2R they are set to: $\alpha_0 = 100$ (used only for the ADRC approach), $\alpha_1 = 2000$, and $\alpha_2 = 30000$. In the case of TRAS they are chosen as: $\beta_0 = 40$ (used only for the ADRC

approach), $\beta_1 = 2400$, $\beta_2 = 32000$, and $\beta_3 = 160000$. The unknown systems design parameters are set in both cases as[3]: $\hat{b}_1 = \hat{b}_2 = 1$.

B. Results for R2R

In the performed experiments, the task is to track the desired sinusoidal signal $y_{ref} = \sin(0.5t) + 5.5\text{V}$. A simple proportional state feedback controller is used with its gain set to $k_p = 15$. A third order ESO is proposed for the first order R2R system from (17), where the first extra state variable represents the *integral state* and the second stands for the estimation of *total disturbance*. The control signal is limited to $u_{max} = \pm 5\text{V}$ to avoid overexploitation of the DC motor.

Results obtained for the sag length trajectory tracking are presented in Figs. 5-8. As one can notice in Fig. 5, there are no significant differences in the tracking quality between ADRC and ADRC*. Both signals provide fast convergence of the estimation error (less than 1s) but only the ADRC* delivers smooth (almost noise-free) signal profile. In the case of ADRC, the noisy estimation error, together with the high gains of the observer, have their negative influence on the estimation of state variables x_1 (Fig. 6) and x_2 (Fig. 7). One should remember, that these states are fetched back to the system to formulate the state feedback controller and the disturbance-canceling loop (19). Hence, the *smoothness* of the control signal profile is directly related to the states $\hat{x}_1$ and $\hat{x}_2$, as seen in Fig. 8.

C. Results for TRAS

In this test, the main objective is to keep the beam at the desired angle (around the vertical axis). The reference signal is a sinusoidal-type function $\theta_{ref} = \sin(0.05t)\text{rad}$. A proportional-derivative state feedback controller is used with its gains set to $k_p = 3$ and $k_d = 0.1$, respectively. A fourth order ESO is proposed for the second order TRAS system from (21), where the first extra state variable represents the *integral state* and the second stands for the estimation of *total disturbance*. The control signal is limited to $u_{max} = \pm 0.5V$ (normalized value) to avoid the excessive exploitation of the DC motor.

Results obtained for the TRAS beam desired angle tracking are presented in Figs. 9-12. Figure 9 depicts the control quality using ADRC and ADRC*. No noticeable differences can be seen here between these two output signals. The distinction becomes clear when analyzing Figs. 10 and 11, which present the estimation quality of state variables χ_2 and χ_3, respectively. The considered observers return similar estimates of these state variables, however some high frequency noise can be seen for the ADRC method. On the other hand, the estimate obtained with the ADRC* approach has a slight phase lag (due to extra integrating action in the observer). In the discussed control setup, estimates $\hat{\chi}_1$, $\hat{\chi}_2$, and $\hat{\chi}_3$ are used in the state feedback controller (i.e. $\hat{\chi}_1$ and $\hat{\chi}_2$ in the proportional and derivative part of the controller, respectively) and in the loop where the estimated *total disturbance* ($\hat{\chi}_3$) rejects the actual perturbation and other uncertainties that affect the system. As a result, there is a significant difference in the *smoothness* and the level of measurement noise in the control signal applied to the plant, as seen in Fig. 12.

[3]Both $\hat{b}_1$ and $\hat{b}_2$ can be considered as scaling parameters (see eq. (12) since they directly influence the closed-loop behavior of the system. In both of the experiments these parameters are chosen empirically with a goal to provide fast output convergence with minimum overshoot effect.

V. Conclusions

In this work, the measurement noise attenuation technique was investigated and experimentally verified in two real environment applications. The proposed approach was implemented in the concept of the Active Disturbance Rejection Controller and compared with its classic version. It was shown, that by introducing a virtual state variable to the plant model, the user can improve the noise rejection of the high-gain observer. The method allows user to safely set higher gains of the observer, thus improve the estimation convergence time and accuracy, without making the controller less energy-saving.

Future work will be devoted to providing a thorough analysis of the presented noise reduction method (e.g. convergence proof of the observer estimation error), a discussion about precise conditions under the described technique works, as well as proposing an objective and reliable method of comparing observers of different orders.

References

[1] K. K. Busawona, P. Kaboreb, Disturbance attenuation using proportional integral observers, International Journal of Control, Volume 74, Issue 6, pp. 618–627, 2001

[2] J. Han, From PID to Active Disturbance Rejection Control, IEEE Transactions on Industrial Electronics, Volume 56, Issue 3, pp. 900–906, 2009

[3] L. B. Freidovich, H. K. Khalil, Robust Feedback Linearization using Extended High-Gain Observers, IEEE Conference on Decision and Control, pp. 983–988, San Diego, 2006

[4] R. Madonski, P. Herman, An Experimental Verification of ADRC Robustness on a Two Rotor Aerodynamical System, IEEE International Symposium on Industrial Electronics, pp. 859–863, Gdańsk, 2011

[5] R. Madonski, M. Przybyla, M. Kordasz, P. Herman, Application of Active Disturbance Rejection Control to a Reel-to-Reel System Seen in Tire Industry, IEEE Conference on Automation Science and Engineering, pp. 274–278, Triest, 2011

[6] D. L. Martinez-Vazquez, A. Rodriguez-Angeles, H. Sira-Ramirez, Robust GPI observer under noisy measurements, 6thInternational Conference on Electrical Engineering, Computing Science and Automatic Control, CCE 2009, art.no.: 5393403

[7] M. Michałek, ZB2 - Laboratory setup user's manual (internal report, in Polish), Chair of Control and Systems Engineering, Poznań University of Technology, 2008

[8] A. Radke, Z. Gao, A Survey of State and Disturbance Observers for Practitioners, American Control Conference, pp. 5183–5188, Minneapolis, 2006

[9] A. Rahideh, M. H. Shaheed, Mathematical Dynamic Modelling of a Twin Rotor Multiple Input-Multiple Output System, Proc. IMechE, Part I: Journal of Systems and Control Engineering, Volume 221, pp. 89–101, 2007

[10] H. J. Sussmann, P. V. Kokotovic, The peaking phenomenon and the global stabilization of nonlinear systems, IEEE Transactions on Automatic Control, Volume 36, Issue 4, pp. 424–440, 1991

[11] Q. Zheng, L. Gao, Z. Gao, On Stability Analysis of Active Disturbance Rejection Control for Nonlinear Time-Varying Plants with Unknown Dynamics, IEEE Conference on Decision and Control, pp. 3501–3506, New Orleans, 2007

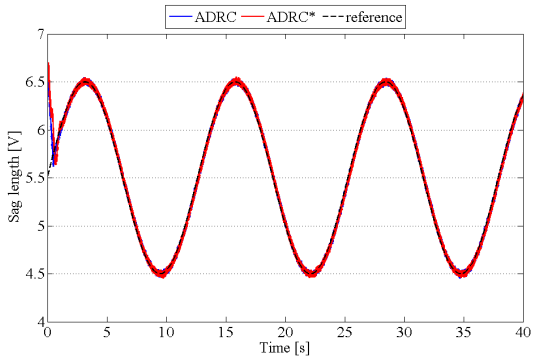

Fig. 5. R2R: sag length trajectory tracking with ADRC and ADRC*.

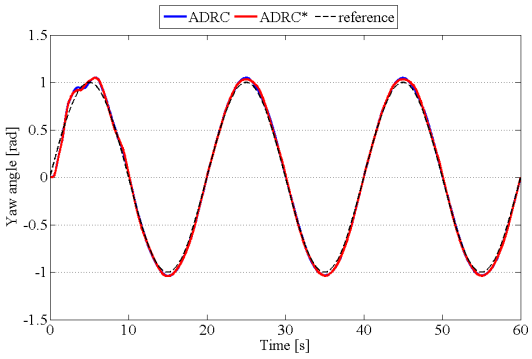

Fig. 9. TRAS: yaw angle trajectory tracking with ADRC and ADRC*.

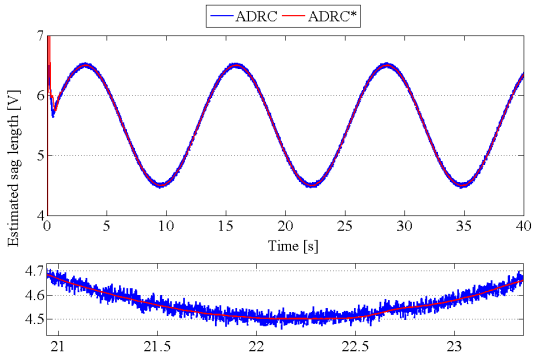

Fig. 6. R2R: estimation of state x_1 with ADRC and ADRC*.

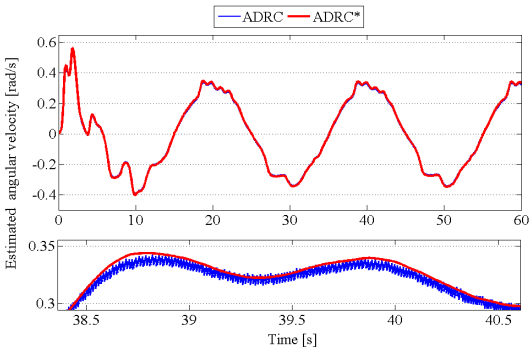

Fig. 10. TRAS: estimation of state χ_2 with ADRC and ADRC*.

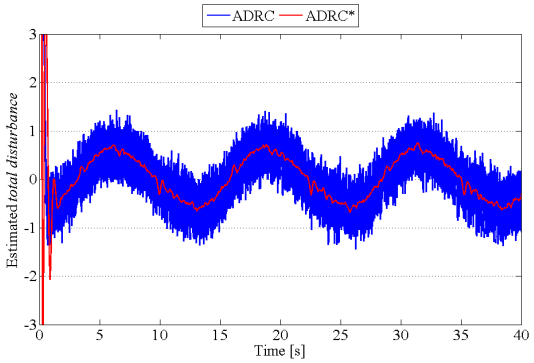

Fig. 7. R2R: estimation of *total disturbance* with ADRC and ADRC*.

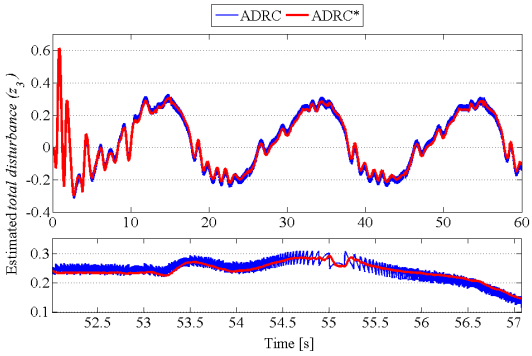

Fig. 11. TRAS: estimation of *total disturbance* with ADRC and ADRC*.

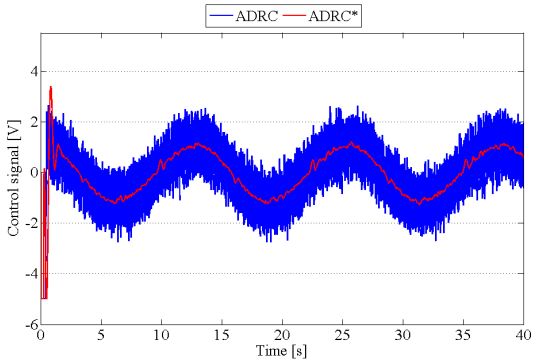

Fig. 8. R2R: control signal with ADRC and ADRC*.

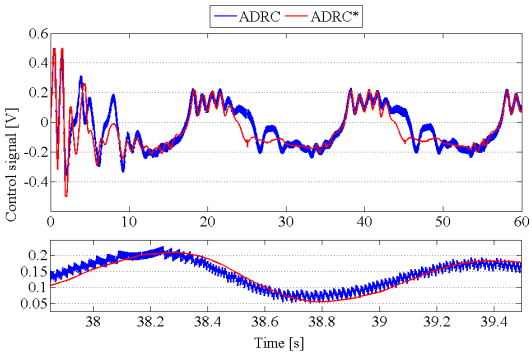

Fig. 12. TRAS: control signal with ADRC and ADRC*.